3rd URSI AT-AP-RASC, Gran Canaria, 29 May – 3 June 2022

Compact Frequency Reconfigurable UWB Monopole Antenna Loaded with Parasitic Line for Wide Stopband

Rushiraj Jawale* and G. Shrikanth Reddy
School of Computing and Electrical Engineering,
Indian Institute of Technology(IIT) Mandi,
Himachal Pradesh, India
*jawalerushiraj@gmail.com

Abstract

This paper presents a frequency reconfigurable monopole antenna using a parasitic line which behaves as a half wavelength resonator. The proposed antenna uses a parasitic line near the partial ground plane of the antenna which can control the stopband frequency with the help of two p-i-n diodes. This is a simple technique and can be used with any printed monopole antenna. A truncated elliptical-shaped monopole antenna with a parasitic line is designed for proof of concept. The antenna gives a UWB band (3-10 GHz) when p-i-n diodes are OFF and a sub-6 GHz band (3.2-5.5 GHz) when p-i-n diodes are ON. The antenna is fabricated on FR-4 substrate and measured for its VSWR and radiation characteristics, it exhibits an omnidirectional radiation pattern, and > 70% efficiency and peak realized gains of 3.2 dBi and 2.2 dBi in UWB and sub-6 GHz bands respectively and is suitable for use in UWB and sub-6 GHz wireless systems.

1 Introduction

Printed monopole antennas [1] are popular due to their compactness and ultra-wide bandwidth. Since the FCC allocated the spectrum from 3.1 - 10.6 GHz for UWB communication, printed monopole antennas have been studied extensively. However, owing to their ultra-wide bandwidth, these antennas cause interference to other wireless technologies such as WLAN, WiMax, etc. In order to minimize the interference, band-notched UWB antennas gained popularity among researchers and various such antennas were reported over the years [2], [3]. But with the upcoming technologies targeting the sub-6 GHz bands such as 5G and cognitive radio and UWB being implemented in smartphones, there is a need to create antennas that can cater to both UWB and sub-6 GHz bands. Printed monopole antennas are a good candidate as they can cover the large bandwidth requirement of UWB and sub-6 GHz bands, provided the frequency band above 6-GHz is suppressed with the help of a proper reconfigurable structure. To switch between the UWB band (3.1-10.6 GHz) and sub-6 GHz band (3.1-6 GHz), a wide stopband structure is needed that can suppress the higher band (6-10GHz) of the UWB monopole antenna. Recent works show methods such as varactor loaded SRR [4], reconfigurable SRRs [5] and monopole antenna with multiple slots [6] which provide narrow band notches and may not be suitable for use with all the monopole antennas.

This paper presents a simple technique that can create a wide stopband. The UWB monopole antenna is loaded with a parasitic line coupled with the partial ground plane of the antenna which gives a wide stopband. Further, with the help of electronic switches such as p-i-n diodes, the structure can be reconfigured such that the antenna can operate in two bands - UWB and sub-6 GHz. The novelty aspects of this design are- It is a general technique that can be used with any printed monopole antenna. It does not affect the antenna performance such as efficiency and radiation characteristics.

2 Antenna Design

The antenna is designed on FR-4 substrate with εr = 4.3, $\tan\delta$ = 0.025 and thickness = 0.8 mm. The antenna shown in Figure 1 consists of a truncated elliptical radiator with a = 12 mm, b = 10 mm, c = 4 mm and a partial ground plane of L_2 = 13.5 mm. A step tapered 50 Ω line with

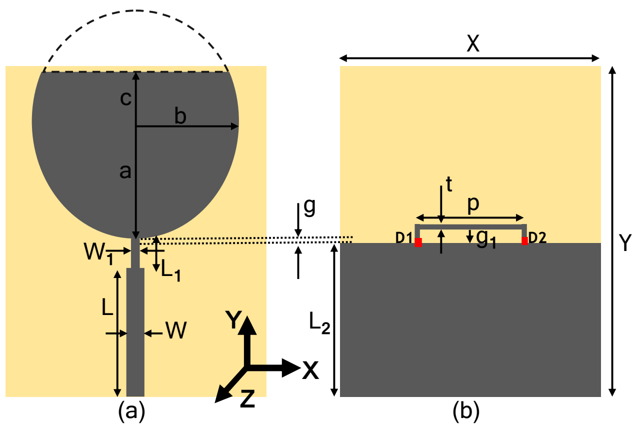

Figure 1. Antenna Structure

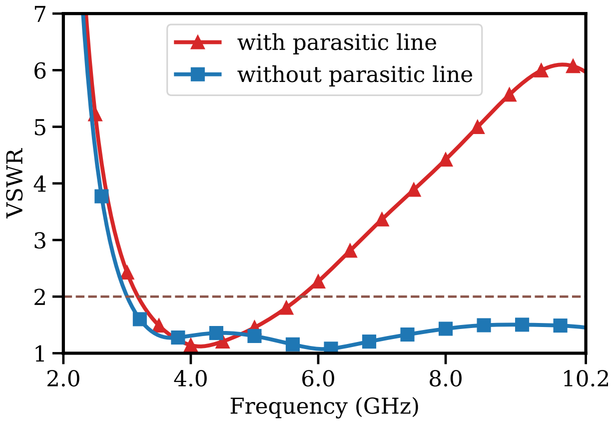

Figure 2. VSWR plot with and without parasitic line connected to the ground plane

dimensions, L = 12.2 mm, W = 1.5 mm, L_1 = 1.8 mm , W_1 = 0.6 mm is used to feed the antenna to get good impedance matching. The gap between the radiator and ground plane is g = 0.5 mm. The overall size of the antenna is X $\times$ Y = 24 $\times$ 31 mm^2. The VSWR plot of the UWB antenna is shown in Figure 2. The proposed structure is simulated in CST Microwave Studio software.

Next, a parasitic line with p = 9 mm and t = 0.3 mm is placed at a distance of g_1 = 0.6 mm from the partial ground plane of the antenna. This parasitic line is connected to the ground plane and the VSWR obtained is shown in Figure 2. It can been seen that when the parasitic line is connected to the monopole antenna the bandwidth of the antenna reduces to the sub-6 GHz band of 3-5.5 GHz from 3-10 GHz. Two p-i-n diodes can be placed near the line to control the connection of the parasitic line with the ground plane depending upon the forward/reverse (ON/OFF) condition of the diodes and a change in the bandwidth of the antenna can be obtained.

The p-i-n diode used in the proposed design is MADP-000907-14020P by MACOM. As per the data-sheet [7] of the diode, it is modelled as a resistor of 7 Ω in the forward bias (ON) and a capacitor of 0.025 pF in reverse bias (OFF) condition. The figure 3 shows the equivalent circuit of the p-i-n diode in OFF (Figure 3a) and ON (Figure 3b) states.

3 Working Principle

In order to understand the working principle of the parasitic line, the $\vec{H}$ field, surface current distribution and the

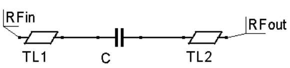

(a) OFF State

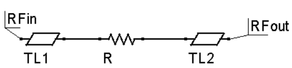

(b) ON State

Figure 3. p-i-n diode equivalent circuit

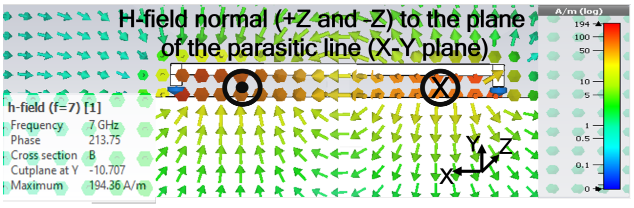

Figure 4. $\vec{H}$ field lines at 7 GHz

impedance are studied.

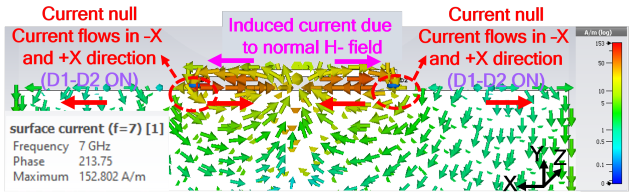

Figure 5. Surface current at 7 GHz for ON case showing induced current

3.1 Excitation of the parasitic line

The $\vec{H}$ field is observed with the inclusion of the parasitic line in the ground plane. From Figure 4, it can be observed that the $\vec{H}$ field is normal to the plane of the parasitic line. The magnetic field lines cross the parasitic line and induce an emf which causes an alternating current to flow through the parasitic line and the direction of the current can be determined using the right hand thumb rule. From the Figure 4 it can be seen that for the left half of the antenna the $\vec{H}$ field lines are in the *+Z* direction denoted by $\odot$ and for the right half, the field lines are in *-Z* direction denoted by $\otimes$. Hence, by using the right hand thumb rule, the direction of the current in the left side is in the *+X* direction whereas current in the right half is towards the *-X* direction. This induced current is then fed into the ground plane of the antenna which creates two "nulls" where the current reverses it direction. The same can be seen in Figure 5.

3.2 Stopband mechanism

From the impedance plot in Figure 6, it can be observed that for the OFF case the magnitude of the real part of impedance $|Z_{\text{real}}|$ and the imaginary part $|Z_{\text{img}}|$ do not show much deviation from 50 Ω and 0 Ω respectively indicating that the antenna essentially behaves as a radiator matched to 50 Ω port. However, for the ON case, $|Z_{\text{img}}|$ shows a inductive reactance from 6- 8 GHz and a capacitive reactance after 8 GHz. At 7.8 GHz, $|Z_{\text{img}}|$ = 0 which denotes the resonance frequency and exhibits pure resistive behaviour with $|Z_{\text{real}}|$ = 211 Ω. The total length of the line (p) = 9 mm is equal to $\lambda g/2$ at 7.8 GHz ($\lambda g, 7.8GHz$ = 18.55 mm) indicating that this line behaves as a half wavelength resonator. From the above study, it can be observed that the parasitic line creates a band stop response with a wide stopband. The bandwidth of the stopband can be further

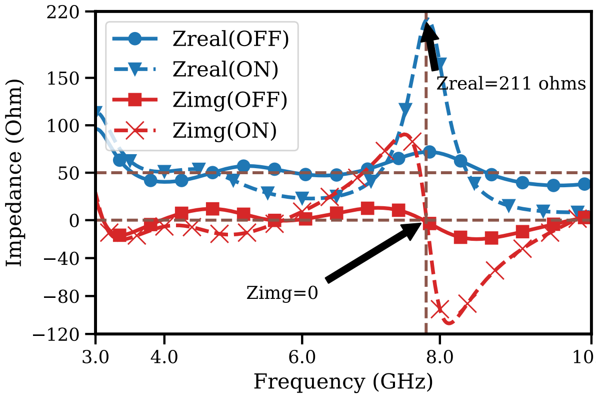

Figure 6. Impedance vs Frequency response for ON and OFF cases

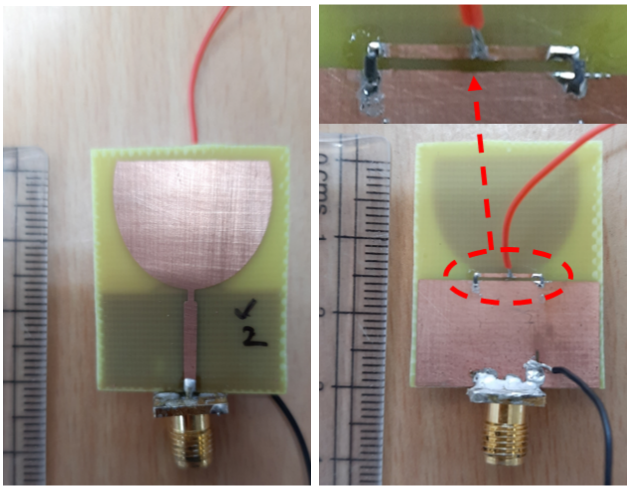

(a) Antenna Top **(b)** Antenna Bottom

Figure 7. Fabricated Prototype

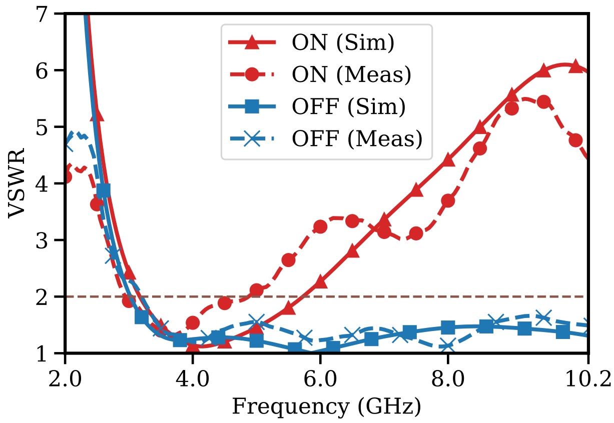

Figure 8. VSWR Plot

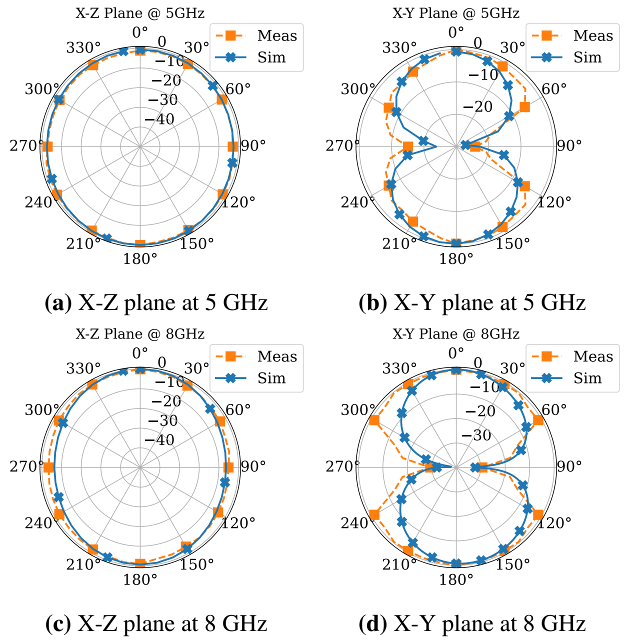

(a) X-Z plane at 5 GHz **(b)** X-Y plane at 5 GHz

(c) X-Z plane at 8 GHz **(d)** X-Y plane at 8 GHz

Figure 9. Measured and simulated radiation pattern for 5 GHz and 8 GHz

controlled by changing the Q factor of the resonator, which depends on the parasitic line thickness and the gap between the ground plane and the parasitic line.

4 Measurement Results

4.1 Antenna Fabrication

A prototype of the proposed structure shown in Figure 7 is fabricated on FR-4 substrate of 0.8 mm thickness and $\varepsilon r = 4.3$ and $\tan\delta = 0.025$ using the UV photolithography process. Two p-i-n diodes (D1 and D2) are hand soldered in the gaps and wires are soldered for biasing the diodes.

4.2 VSWR and Radiation Pattern

The fabricated prototype is measured for it's VSWR and radiation characteristics. For the OFF condition, 0V DC voltage is applied to the p-i-n diodes and for the ON condition, a 1.3V DC voltage is applied.

From the Figure 8 it can be seen that the measured VSWR results agree with the simulation results. A slight shift in the VSWR for the D1-D2 ON case could be due to the effect of biasing wires soldered to the antenna. The radiation pattern for the antenna is measured in a anechoic chamber environment. The measured vs simulation radiation patterns in the X-Z and X-Y planes at 5 and 8 GHz are shown in Figure 9. The measured pattern agrees with the simulated results and the antenna exhibits an omnidirectional pattern.

4.3 Efficiency and Gain

From the efficiency response in Figure 10, it is observed that the proposed antenna has an in-band efficiency of > 80% in the entire UWB band and > 70% for the sub-6GHz band and good out-of-band performance with reduced efficiency in the stopband.

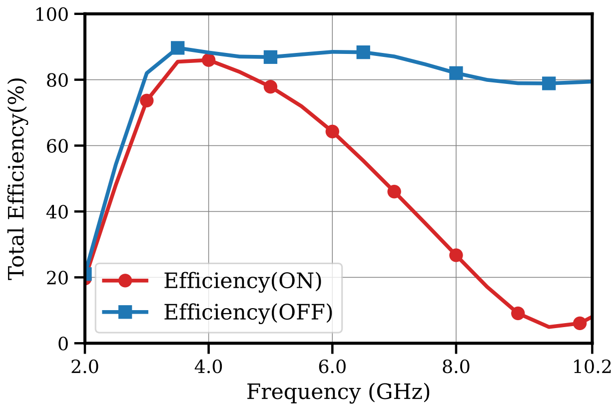

Figure 10. Efficiency response of the proposed antenna

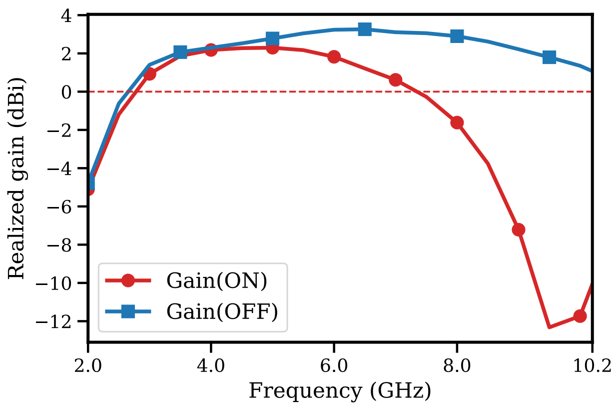

Figure 11. Gain response of the proposed antenna

The realized gain response shown in Figure 11 shows a peak realized gain of 3.2 dBi in the UWB band and 2.2 dBi in the sub-6 GHz band. The gain and efficiency both fall sharply in the stopband indicating a good stopband performance of the antenna.

5 Conclusion

A frequency reconfigurable printed monopole antenna is designed which can be reconfigured to work in two frequency bands - UWB(3-10 GHz) and sub-6 GHz(3.2-5.5 GHz) using a simple method of a $\lambda g/2$ parasitic line resonator that can provide a wide stopband. This method can be used with any printed monopole antenna. The proposed antenna is fabricated and measured for VSWR and radiation characteristics. The antenna exhibits an omnidirectional radiation pattern with efficiency >70% in both the bands and peak realized gains of 3.2 dBi and 2.2 dBi in the UWB and sub-6 GHz bands respectively. The antenna is suitable for sub-6 GHz 5G and UWB systems.

6 Acknowledgements

We acknowledge the support of DST-SERB, Govt. of India for the financial help .

References

[1] N. P. Agrawall, G. Kumar and K. P. Ray, "Wide-band planar monopole antennas," *IEEE Transactions on Antennas and Propagation*, vol. 46, no. 2, pp. 294-295, Feb. 1998, doi: 10.1109/8.660976.

[2] J. Y. Siddiqui, C. Saha and Y. M. M. Antar, "Compact Dual-SRR-Loaded UWB Monopole Antenna With Dual Frequency and Wideband Notch Characteristics," *IEEE Antennas and Wireless Propagation Letters*, vol. 14, pp. 100-103, 2015, doi: 10.1109/LAWP.2014.2356135.

[3] G. S. Reddy, A. Kamma, S. K. Mishra and J. Mukherjee, "Compact Bluetooth/UWB Dual-Band Planar Antenna With Quadruple Band-Notch Characteristics," *IEEE Antennas and Wireless Propagation Letters*, vol. 13, pp. 872-875, 2014, doi: 10.1109/LAWP.2014.2320892.

[4] K. Sathish, C. Saha, D. Sarkar, J. Y. Siddiqui and y. antar, "Varactor-Controlled SRR-Integrated Frequency-Reconfigurable Multifunctional Vivaldi Antenna: A Proposed Concept.," *IEEE Antennas and Propagation Magazine*, doi: 10.1109/MAP.2021.3106893.

[5] Saha Chinmoy, Siddiqui Jawad Y., Freundorfer A. P., A Shaik, Latheef, Antar, Y. M. M., "Active Reconfigurable Ultra-Wideband Antenna With Complementary Frequency Notched and Narrowband Response," *IEEE Access*, **8**, 2020, pp. 100802-100809, doi: 10.1109/ACCESS.2020.2997933.

[6] Nan Jingchang, Zhao Jiuyang, Gao Mingming, Yang Wendong, Wang Minghuan and Xie Huan, "A Compact 8-States Frequency Reconfigurable UWB Antenna," *IEEE Access*, **9**, 2021, pp. 144257-144263, doi:10.1109/ACCESS.2021.3122250.

[7] MACOM, MADP-000907-14020P